Environmental Earth Sciences (2021) 80:97
https://doi.org/10.1007/s12665-021-09396-x

ORIGINAL ARTICLE

Evaluation of seismic site classification for Kahramanmaras City, Turkey

Dalia Munaff Naji[1] · **Muge K. Akin**[2] · **Ali Firat Cabalar**[3]

Received: 5 May 2020 / Accepted: 14 January 2021 / Published online: 28 January 2021

Abstract

This paper presents a study on the seismic site classification map using the geophysical tests in Kahramanmaras city located at a place where African, Anatolian, and Arabian plates meeting in southern-central Turkey. Generating seismic site classification maps in accordance with National Earthquake Hazards Reduction Program (NEHRP) has become a more significant criterion for earthquake hazard estimations. The SPT-N values obtained from the field studies at 287 boreholes within the upper 30 m were used to describe the subsurface conditions in the region. The shear wave velocity (V_S) values in the study area were obtained by implementing Multichannel Analysis of Surface Waves (MASW) and Microtremor Array Method (MAM) measurements tests. An approach proposed by Boore (Boore, Bull Seismol Soc Am 94:591–597, 2004) for the cases where the V_S measurements do not reach 30 m depth has also been adopted by correlating the shallow shear wave velocity with V_{S30}. The resulting site classification maps estimate that the study area is predominantly classified as soil site class C, while the small areas were rarely classified as soil site class D and B. Furthermore, a systematic analysis based on a comparative study of the present research and the published correlations for seismic site classification with V_{S30} values has been carried out using Geographical Information System (GIS). Evidently, the V_{S30} based seismic site classification maps could be effectively used by researchers and engineers for the purpose of land-use planning and urban development in earthquake-prone regions.

Keywords SPT-N · Shear wave velocity · Seismic site classification · Microtremor · MASW

Introduction

Engineering properties of soils have a considerable influence on the amplitude and period of bedrock movement when the seismic waves arrive in the ground surface. This phenomenon is defined as the seismic site effect. Evaluation of Seismic Site Classification (SSC) at a specific area is generally carried out by using SPT-N or shear wave velocity (V_S) values for the purpose of various reasons including land-use planning, urban development, site response, and microzonation studies in an earthquake prone regions (Pitilakis 2004; Akin et al. 2013). Actually, the shear wave velocity, V_S is an important parameter to determine the dynamic response of soils, liquefaction potential, and soil profile (Seed et al. 1981; Leparoux et al. 2000; Thitimakorn and Channoo 2012). Another significant parameter in estimating dynamic responses of the soils is the mean shear wave velocity for the soil in the upper 30 m of the ground surface (V_{S30}), which is obtained by dividing 30 m with the required time for the waves to pass the surficial 30 m (Dobry et al. 2000; BSSC 2001; Boore 2004). Site classifications using the V_{S30} values are needed for specifying site response in regression formulas (Boore et al. 1997, 2011; Thompson and Wald 2016) and for generating site classification maps based on the National Earthquake Hazard Reduction Program (NEHRP) soil classification system (Wills et al. 2000; Rodriguez-Marek et al. 2001).

✉ Ali Firat Cabalar
cabalar@gantep.edu.tr

Dalia Munaff Naji
daliamunaff@gmail.com

Muge K. Akin
muge.akin@agu.edu.tr

[1] Department of Civil Engineering, Al-Mustansiriyah University, Baghdad, Iraq

[2] Department of Civil Engineering, Abdullah Gul University, Kayseri, Turkey

[3] Department of Civil Engineering, University of Gaziantep, Gaziantep, Turkey

Following the 17 August Izmit ($M_w = 7.4$), and 12 November Duzce ($M_w = 7.1$) earthquakes that struck Turkey in 1999, the earthquake hazards in Turkey has become a great concern. Kahramanmaras is located in a region where African, Anatolian, and Arabian plates meet in southern-central Turkey. This paper reports what is thought to be the first study ever carried out to define the major site classes of soil in the region using V_{S30} estimates that will help to predict the soil response for future seismic events. To prepare the SSC maps of the study area, a large number of V_S records reported by Akil and Ecemis (2011) and Ozmen et al. (2017) were utilized. Eventually, this paper aims to investigate the response of soils in Kahramanmaras area within the zone of influence of the Bitlis Thrust Zone, East Anatolian Fault Zone (EAFZ), and the Dead Sea Fault Zone (DSFZ) in southern-central Turkey. Investigation on the study area has been accomplished by using shallow seismic wave tests of Multichannel Analysis of Surface Waves (MASW), Microtremor Array Method (MAM) and drilled boreholes. This research proposes a series of equations for different depths ranging from 10 to 24 m to estimate the V_{S30} values for a site without any fieldwork in the study area. Consequently, the paper presents a pioneering study on a subject that should be of great benefits for further use by researchers.

Study area

Kahramanmaras, located at 37.75° N 36.95° E and 67 m elevation, is a city with more than a million population in the southern-central Turkey and lies in one of the most seismically active regions in the country (GDDA 2019) (Fig. 1). The city and its vicinity are located in an area where the potential of destructive earthquakes is high due to the influence of the EAFZ and the DSFZ (Biricik and Korkmaz 2001). The city has an area of 25.622 hectars, and the urban settlement is located within the Kahramanmaras thrust system (Akil and Ecemis 2011) (Fig. 2).

Geological setting of the study area

The Kahramanmaras basin is located in southern central Turkey, where the tectonic plates of Africa, Arabia and Anatolia meet. The collision of Arabian and Eurasian plates along the Bitlis suture zone over the years caused a trough to be formed in front of the thrust sheets, as a result thick alluvial sediment were deposited there (Sengor and Yilmaz 1981; Perincek and Kozlu 1984; Karig and Kozlu 1990; Yilmaz 1993; Husing et al. 2009). Hence, Kahramanmaras is a tectonic-based alluvium plain whose boundaries are under the control of fault lines. The length of Kahramanmaras plain lying between Cimen and Ahir Mountains is 40 km, and the width from north to south is nearly 20 km. Gul et al. (2005) suggest that limestone and claystone deposits can be found in the basin, on top of which lies shallow marine deposits. In the Kahramanmaras basin, geological units representing a period from Cambrian to the present day are observed. In the area of Kahramanmaras and its near north, Cambrian, Triassic, Jurassic, Cretaceous, Tertiary and Quaternary units are outcrops (Fig. 3). The oldest unit in the study area is the Cambrian Koruk formation and the latest units are Quaternary alluvial deposits.

A geological map was prepared in this study (Fig. 4) depending on the information obtained from the observation

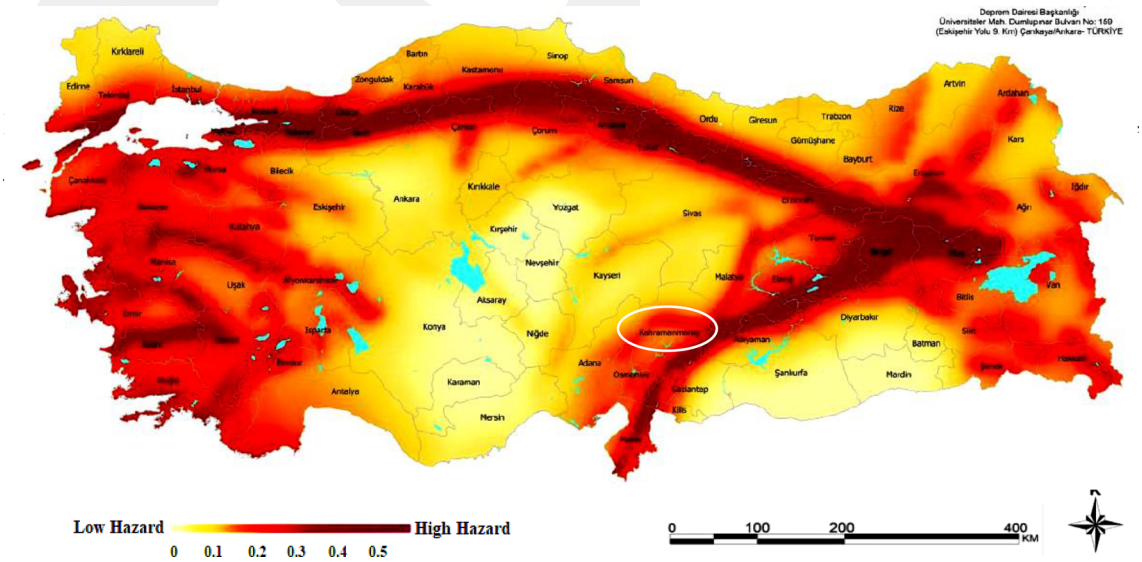

Fig. 1 The Seismic Hazard Map of Turkey (GDDA 2019)

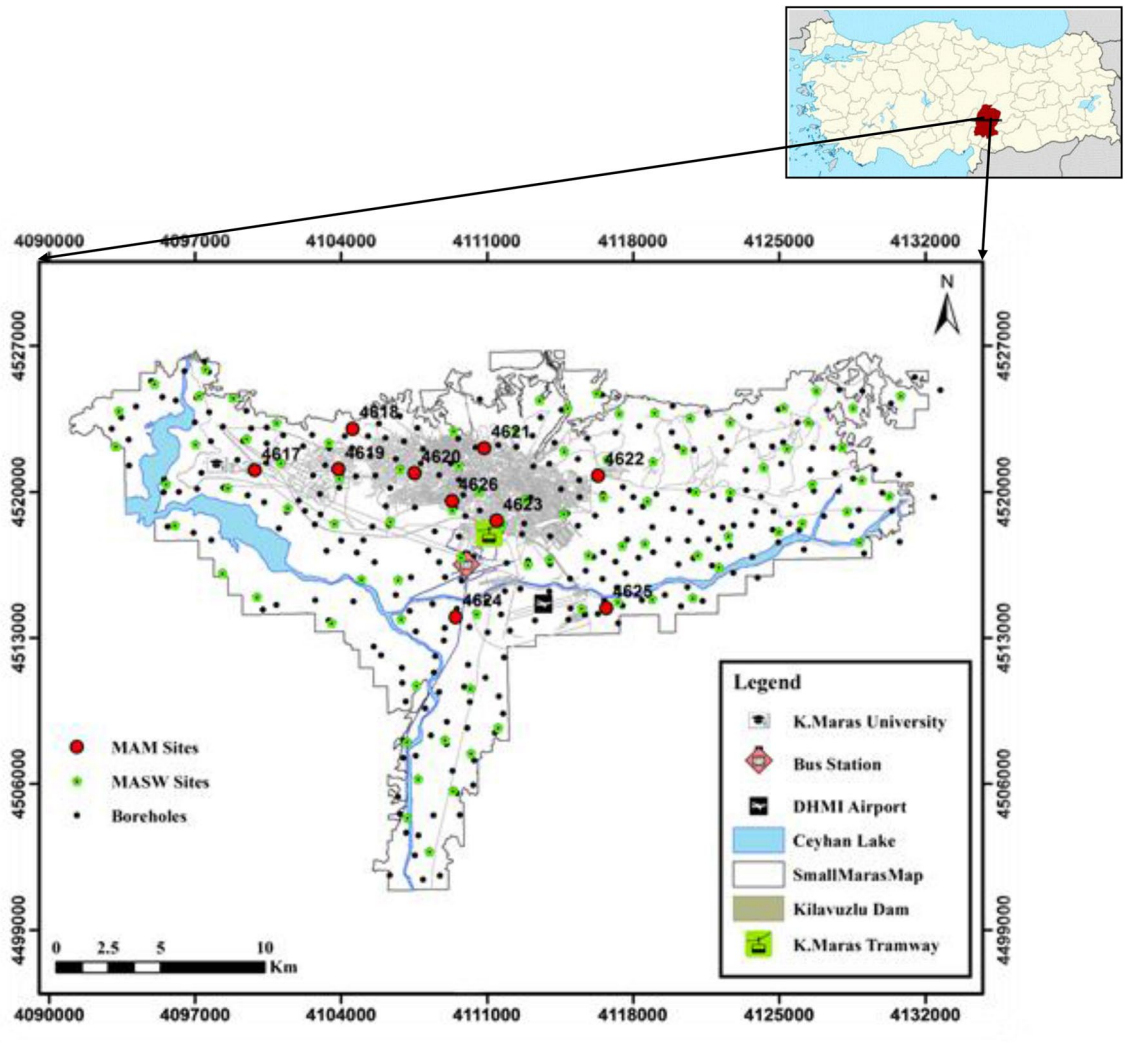

Fig. 2 Location map of the study area with distribution of V_S sites and boreholes in Kahramanmaras city (Akil and Ecemis 2011; Ozmen et al. 2017)

points at different parts in the study area performed by the Municipality of Kahramanmaras. The map illustrates the major geological units forming the study area. The Ahirdagi formation (green zones in the map) is observed in the north of the study area and is generally tectonic in contact with other units and it is of Limestone formation. The unit is generally rigid and compact and is very strong-durable. The carbonate rocks belonging to the Ahirdagi member of Midyat Formation is more durable in terms of ground. It is suggested to build on the skirts of Ahirdagi in the north of Kahramanmaras.

The Pinarbasi formation (yellow zones) spreads along with the southern skirts of Ahirdagi and borders with Golbası formation in the form of pressure ridges with the effect of thrusts in the southernmost. The formation, which is widely seen in the urban area, continues until the easternmost part of the study area. The Pinarbasi formation consists of different types of pebbly and blocky pebbles, such as angular, stony, variable size, poorly bedded, predominantly limestone deposits. The unit is mostly medium-loose fastened with carbonate cement. The Golbası formation (blue zones) is starting from Kavlaklı in the western part of the study area. It is composed of pebble, mud and sand intermediate additives from river sediments and is horizontally bedded. Yavuzeli Basalts give widespread outcrops on the ridges to the west of Ahirdagi Mountain.

The combined alluvial deposits (red zones) in the basin form the flat part of the city. Alluviums are composed of undisturbed gravel, block, sand, silt, clay and shaft, usually located in river valleys. The alluvium material is transported by streams located in the northern part of the plain. Alluvial sediments observed in many streams, including Erkenez stream and Aksu Stream. Alluvial sediments observed in the southeast of the study area has a lithology containing gray,

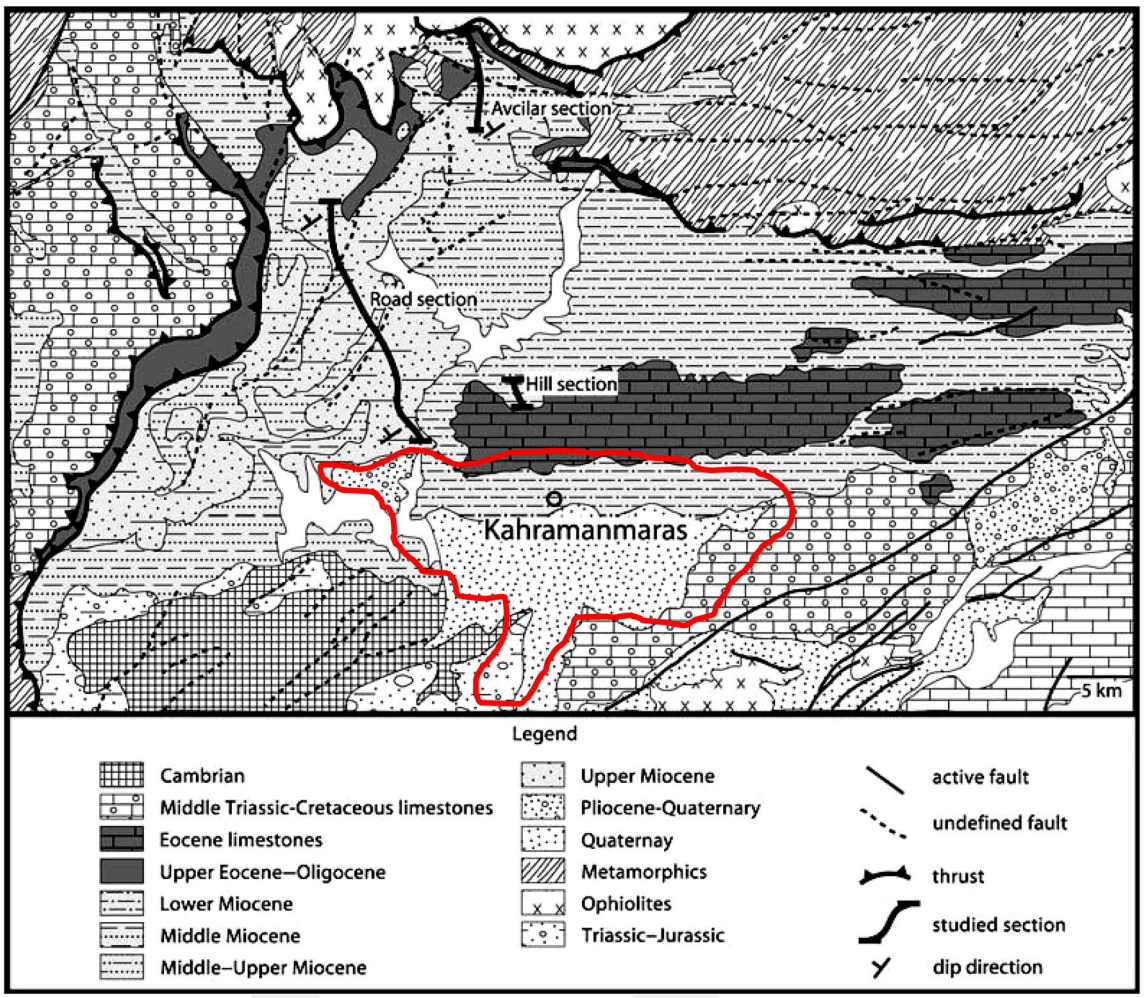

Fig. 3 Location and detailed geological map of Kahramanmaras area (Husing et al. 2009)

light gray colour, polygenic grained, mostly gravel and light brown colour sand, and sometimes clay levels (Korkmaz 2000). It is formed by the accumulation of alluviums on the basin of Ceyhan River and Aksu Stream. The old Alluvial deposits (orange zones) is observed in the southwestern part of the study area, in a state formed in the south of the Erkenez stream relative to the stream bed.

Seismic activities in the study area

The collision among the Arabian and Anatolian plates created the Kahramanmaras territory. The available structural schemes set the triple junction of Arabia-Anatolia-Africa close to Kahramanmaras (Sengor et al. 1985). Kahramanmaras city is surrounded by active faults of the southern and northern branches of the EAFZ (Amanos segment, Golbasi-Turkoglu segment, Surgu segment, Savrun segment, Cardak segment, Toprakkale segment, and Cokak segment), Kahramanmaras Fault Zone, Engizek Fault Zone, and Narlı segment of the DSFZ (Palutoglu and Sasmaz 2017).

According to Ambraseys and Jackson (1998), Nalbant et al. (2002) and Yilmaz et al. (2006), the Golbası-Turkoglu segment is associated with the largest of the known historical earthquakes occurred along the EAFZ, such as 1114 ($M_w > 7.8$), 1513 ($M_w > 7.4$), and 1893 ($M_w > 7.1$) earthquakes. Hence, 7.3 is the expected magnitude of a possible earthquake or larger along this segment.

Methodology

There are numerous studies correlating certain variables to provide a useful reference for numerical simulations (Goh and Zhang 2014; Zhang et al. 2015, 2020; Zhang and Goh 2015; Zhu et al. 2019; Wengang et al. 2020). One of the surface wave analysis methods to estimate the V_S in a precise way is the MASW method that was pioneered by Park

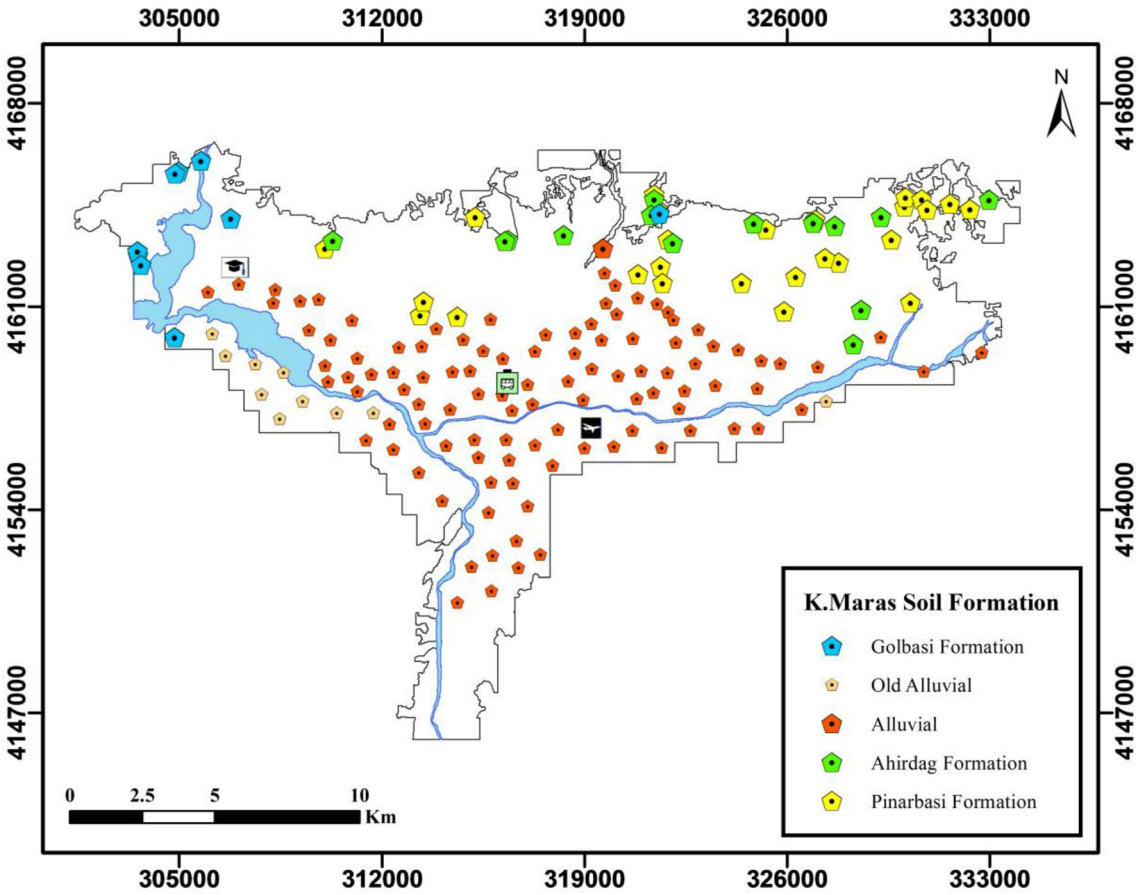

Fig. 4 Major geological units of Kahramanmaras area

et al. (1999). The MASW is a simple method in estimating near-surface V_S profile and has been widely employed to estimate the V_{S30}. It provides accurate results for determining the thickness of soil layers in a profile (Kanli et al. 2006). Phase velocity values at 88 different locations were determined using the MASW method in the study area. The MASW method in the present study consists of a geometrics seismograph with 12 vertical geophones of 4.5 Hz spaced 3 m away from each other. A 9 kg sledgehammer, struck a 30 cm × 30 cm steel plate at the end of the array, was used as a seismic source. The offset distances were taken as 12 m at site point 82, and 18 m at other measurement points, while the sampling interval for recording at all measurement points is 1.0 ms and the recording length is 2 s. Seismic data were evaluated as one-dimensional (1-D) using Surfseis v.2.0 (Choon 2000; Akil and Ecemis 2011). Rayleigh wave velocity values at 88 different locations were determined using the MASW method in the study area. The MASW testing locations are shown in Fig. 2. A plot of phase velocity, which was calculated from the linear slope of each component on the swept-frequency record, versus frequency has been prepared. The V_S has been derived by inverting the dispersive phase velocity of the surface wave. The shear wave velocity profile was calculated using an iterative inversion process that requires the dispersion curve as input. Following the inversion step, the V_S profiles (variation of shear wave velocity with depth) were obtained.

Ozmen et al. (2017) conducted the MAM exploration of shallow S-wave velocity profiles at 28 sites in Hatay and Kahramanmaras (in the southern central Turkey). A total of 12 sites were located in Kahramanmaras province, whilst 10 stations were located in the Kahramanmaras city (Fig. 2). They installed two small arrays by using seven sensors at each site to obtain simultaneous records of vertical microtremors. The Spatial Auto Correlation (SPAC) method was applied to retrieve Rayleigh-wave phase velocities in a 1–30 Hz frequency range. Simultaneous records with seven sensors were obtained over about 10–20 min for each array. The cross spectra for two-station pairs were used to calculate SPAC coefficients at each frequency. Then, these coefficients were averaged to be converted to frequency-dependent phase velocities. High-phase velocities in the entire frequency range were observed at many sites in the study area. The observed phase velocity at each site was inverted to a 1D

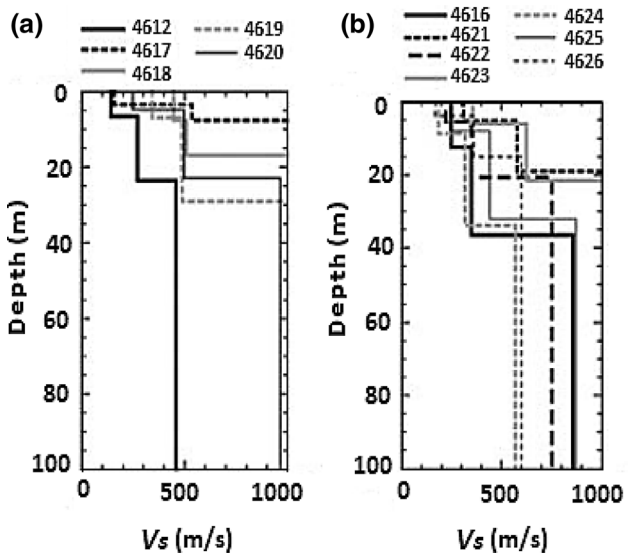

Fig. 5 V_S profiles implemented by the MAM test in the study area (Ozmen et al. 2017)

Table 1 Definition of NEHRP site classes in terms of V_{S30} and N_{30} (BSSC 2003)

Site class	General description	V_{S30} (m/s)	N_{30}
A	Hard rock	>1500	–
B	Rock	$760<V_{S30}\leq1500$	–
C	Very dense soil and soft rock	$360<V_{S30}\leq760$	>50
D	Stiff soil	$180<V_{S30}\leq360$	$15\leq N_{30}\leq50$
E	Soft soil	$V_{S30}<180$	<15

S-wave velocity profile to a depth of 100 m using a hybrid heuristic inversion as shown in Fig. 5. The velocity values from the MAM sites (4617, 4618, 4619, 4620, 4621, 4622, 4623, 4624, 4625, and 4626) as well as the MASW sites have been effectively used for mapping in the present study. Most of the profiles in the study area have top layers with less than 10 m at all sites. The V_S of the top layers were found to be relatively high at many sites in the area. Only three sites (4617, 4624, and 4626) have top layers with V_S values less than 200 m/s (Ozmen et al. 2017).

Seismic site classification

The NEHRP recommends classifying soils into five different categories to specify the effects of the ground amplification and attenuation (Table 1). Determination of site class is based on the mean soil properties in soils up to 30 m depth. The parameters of soil type, blow count (SPT-N), shear wave velocity (V_S) measurements in field, and shear strength (S_u) have been used to identify the engineering characteristics of the soils (FEMA 2010). The SSC can be determined by using 30 m mean shear wave velocity (V_{S30}) values, 30 m mean penetration resistance (N_{30}), and undrained shear strength (S_{u30}) (Borcherdt 1994). Based on V_S and/or SPT-N values in upper 30 m, the averaged shear strength of soil would be estimated by:

$$V_{S30} \text{ or } N_{30} = \frac{30}{\sum_{i=1}^{n}\left(\frac{d_i}{N_i \text{ or } V_{si}}\right)} \quad (1)$$

where d_i is the thickness of the ith layer (m), v_i is the V_S of the ith layer (m/s), N_i is SPT-N values, and n is the strata numbering or the number of V_S values measured within the uppermost 30 m (Boore 2004).

Boore (2004) made a comparative study among four available procedures used to determine the velocity profiles in a field within upper 30 m for the measurements which did not reach 30 m. One of these procedures, for example, suggests extending the lowermost V_S value to 30 m, while another one utilizes the correlations between average velocity with depth d (V_{Sd}) and V_{S30} values. The d is defined as the depth to the base of the measured velocity profile. Hence, the V_{Sd} is evaluated using the formula below.

$$V_S(d) = \frac{d}{tt(d)} \quad (2)$$

The travel time ($tt(d)$) to depth d shown above is obtained by

$$tt(d) = \int_0^d \frac{d_z}{V_S(z)} \quad (3)$$

where $V_{S(Z)}$ is the depth-dependent velocity parameter for each depth increment (dz).

Eventually, Boore (2004) developed a framework using the data obtained at depths less than 30 m over an area to estimate V_{S30} values. To make such estimates, Boore (2004) proposed to extend the V_S of the lowest layer up to 30 m depth or to make a correlation between V_{S30} and average V_S up to the depth of d (V_{Sd}). In general, the method employing correlations gives out the best results on estimating V_{S30}. In the present paper, the authors have used the study by Boore (2004) to estimate the V_{S30} of Kahramanmaras city by correlating the shallow velocity (V_{Sd}) with V_{S30}. In the present research, 15 MASW sites with V_S values up to 30 m depth, and 10 MAMsites with V_S values up to a depth of 100 m, 51 sites with V_S values ranging between 10 and 24 m from MASW method have been investigated. A 21 models with measured V_S values less than 10 m depth has been ignored during this study as stated by Boore (2004). Figure 6 presents some samples

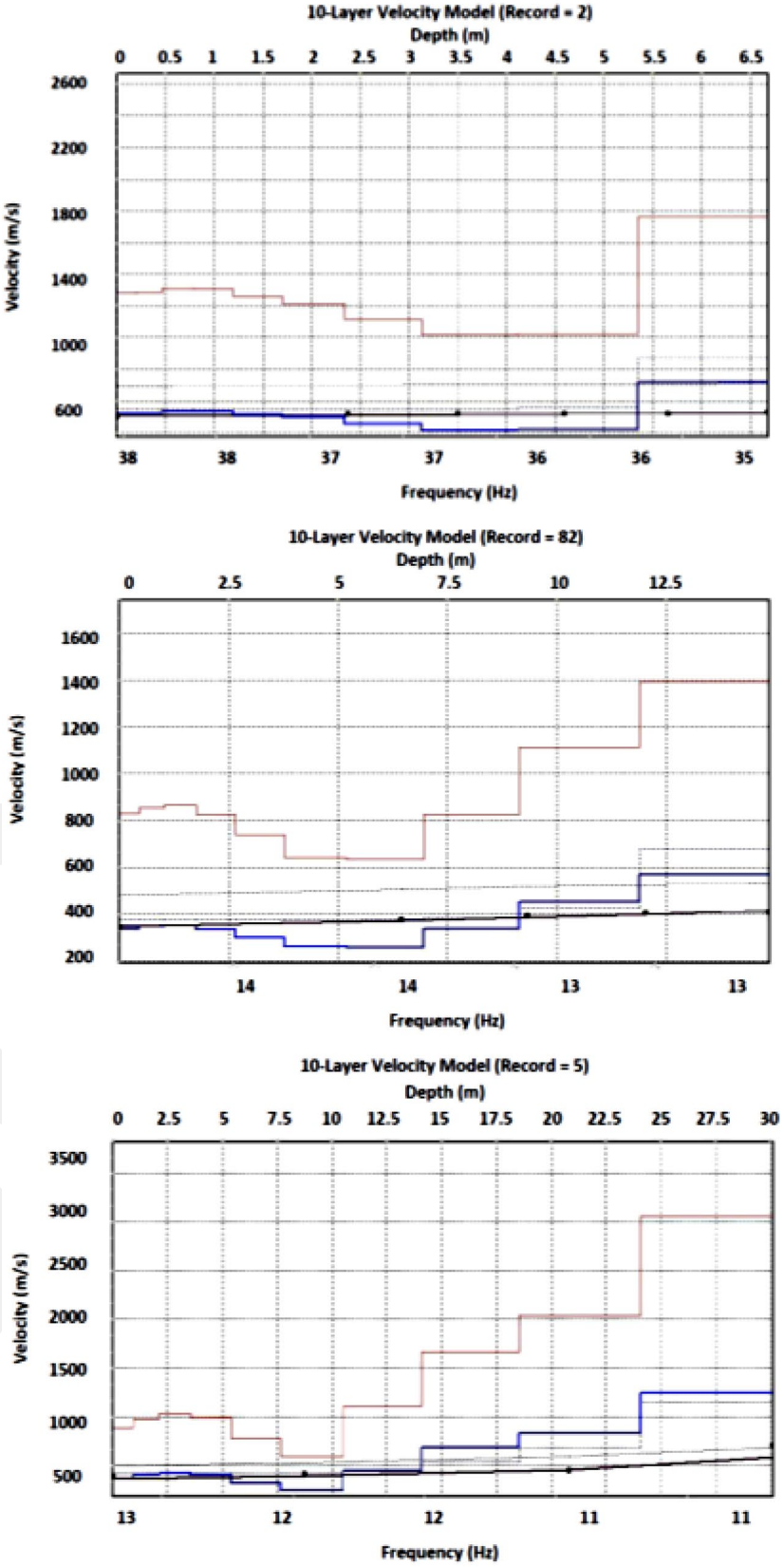

Fig. 6 Recorded shear wave velocity profiles for Kahramanmaras city for stations 2, 82 and 5 with investigated depths of 6.5 m, 15 m and 30 m, respectively (Akil and Ecemis 2011)

of the velocity models for measured MASW in different sites (stations 2, 82, 5) with various depths (6.5 m, 15 m, 30 m) on the study area. The velocity values were found to increase with the increase in depth regardless of their location.

V_{S30} by correlating V_{S30} and V_{Sd}

V_{S30} values of the 25 sites (15 MASW, and 10 MAM sites) in the study area had been measured based on the field studies, whilst those of 51 sites in the study area were estimated using the correlations between these V_{S30} values available over 25 sites and the V_{Sd} values measured at different depths ranging from 10 to 24 m. Actually, it should be kept in mind that the additional 51 and shallow measurements are not from borehole dataset, and the *V*s measurements were collected by the non-invasive MASW. Eventually, 15 different equations for depths ranging from 10 to 24 m with a 1 m increment have been derived using a statistical approach (Statistical Package for the Social Sciences, SPSS) (Fig. 7). In the light of the study by Boore (2004), a linear regression line to describe the relationship between V_{S30} and V_{Sd} for the 25 sites is of the equation form below.

$$\log V_S(30) = a + b \log V_S(d) \quad (4)$$

where a is the explanatory variable and b is the dependent variable. The slope of the line is b, and a is the intercept. Equation 4 has been proposed to estimate V_{S30} for the sites at a depth less than 30 m and larger than 10 m ($10\ \text{m} \le d < 30\ \text{m}$) by employing the V_{Sd} values, thus the NEHRP site class would be able to be assigned. A general view of Fig. 7 shows a lower dispersion associated with high precision by an increment in depth. Regression coefficients (R^2) of Eq. 4 to describe the strength of the relationship between a predictor value and the response are listed in Fig. 7, which also gives out the a and b values. In general, the larger R^2, the better the regression model fits the observations made. It is seen that the correlations proposed were found to be quite reasonable for all depths including the 10 m one, the worst case. As shown in Fig. 7, the theoretical V_{S30} values were estimated by projecting the measured V_{S30} values on the regression line. A close observation on depths ranging from 10 to 17 m given in Fig. 7 reveals that about one third (1/3) of the data points in Fig. 7 (measured V_{S30}) were situated above the regression line indicating an underestimation of V_{S30} compared to the measured one, i.e. measured V_{S30} > theoretical V_{S30}. Another part of the data in Fig. 7 were located below the regression line and their projections denote the overestimation of V_{S30} (measured V_{S30} < theoretical V_{S30}). Relatively, small amount of the values has been taken place on the regression line meaning the coincidence of the measured values with the estimated ones.

V_{S30} map for the study area

The soil profiles for the 25 sites were presented in Fig. 8 where V_{S30} measurements were made in the field. For example, Fig. 8a shows the soil profile for site number 4624 with V_{S30} value of 260 m/s (loose to medium soil). Soil profile described as class D in the upper layer, and C in the lower layer was illustrated in Fig. 8b. Figure 8c represents the soil profile changing from class D to class C, and class B. Actually, the soil class defined in the profile given in Fig. 8f is dominantly classified as C in spite of the presence of various soil classes in this site. Furthermore, the soil is classified as C although there are weak and soft layers named as class E (V_{S30} equals to 150 m/s) along with a depth of 2.7 m in site number 4617. The SSC map has been prepared to indicate the earthquake-prone sites in the study area using the V_{S30} values compiled by means of Geographic Information System (GIS) software that employs Kriging technique (Fig. 9). The V_{S30} values for the extended 51 sites were estimated by using Eq. 4, while those for 25 sites were determined using Eq. 1. The V_{S30} values were found to be varied from 263 to 1086 m/s over entire the study area. According to the NEHRP classification system, 59 sites in the study area were found to be class C (about 78% of the whole study area) with the V_{S30} values changing between 360 and 760 m/s, 11 sites, in particular the northern sections, were classified as B (about 14% of the whole study area) with the V_{S30} values were ranging between 772 and 1086 m/s, and 6 sites were found to be class D (about 8% of the whole study area) with those from 263 to 359 m/sec. The class B soils consist of igneous rocks with overlapped layers of stiff sedimentary rocks and massive metamorphic rocks and conglomerate. Figure 9 displayed the locations of 25 fully measured V_{S30} as coloured circles, and the 51 extrapolated V_{S30} locations as coloured squares. Measured and estimated V_{S30} values for the 25 sites have been compared to evaluate the performance of the regression models developed in the present study. As can be seen from Fig. 10, there is a close relationship between the V_{S30} values measured (Eq. 1) and those estimated using the approach developed here in the present work (Eq. 4). Majority of the data points in the plot areas were found to come close to the best-fit line (1:1) confined by the lines with 1:0.75 and 1:1.34 slopes. In general, there is a larger difference between the V_{S30} values estimated using the approach proposed in the present study and the V_{S30} values measured in relatively shallow depths. However, such difference between the V_{S30} estimated and the V_{S30} measured was found to decrease by substantial increments in depth.

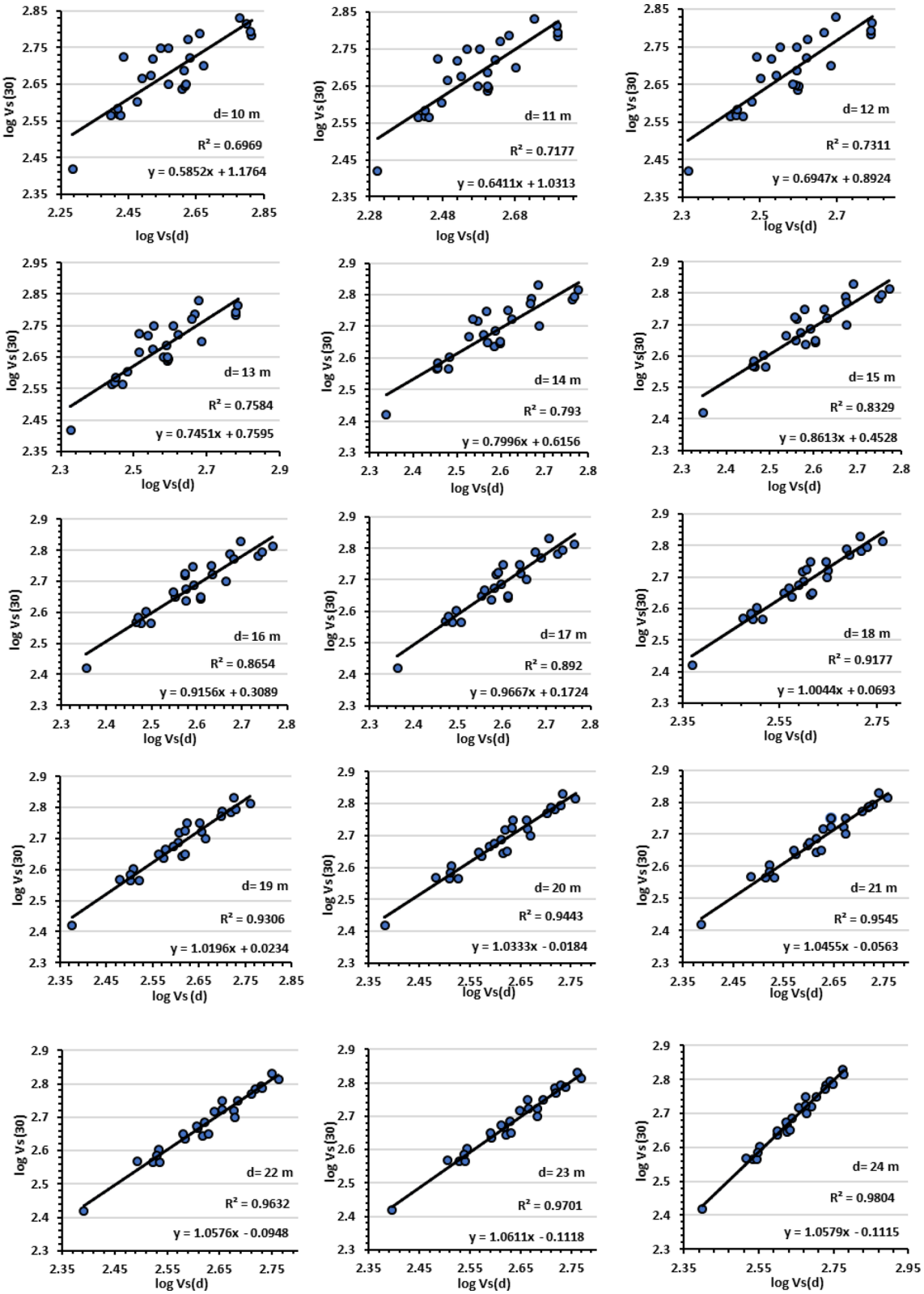

Fig. 7 Regression line suitability to log V_{S30} which is a function of log V_{Sd} for the mentioned depth levels

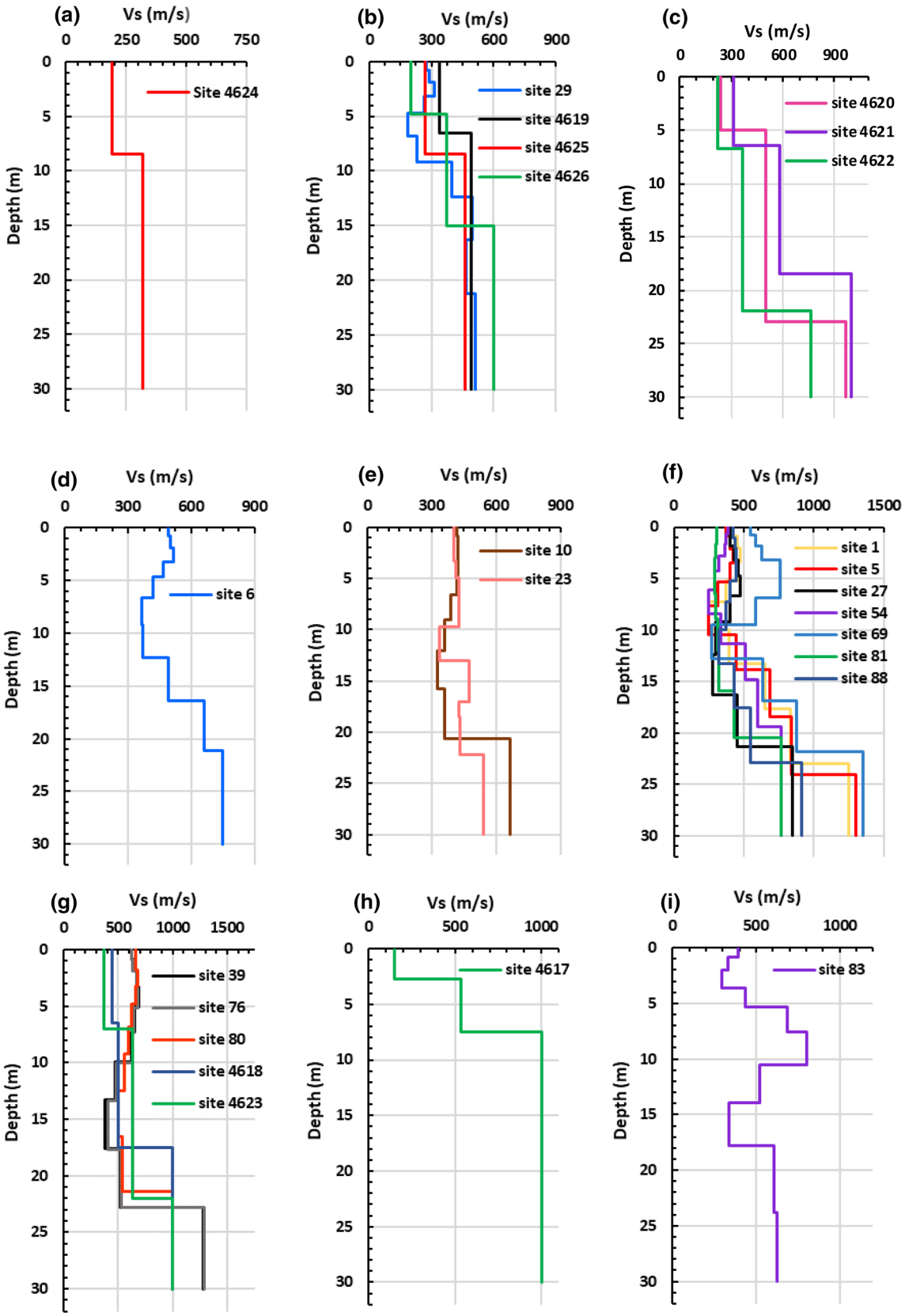

Fig. 8 Transformation of the measured 25 V_S profiles with depth (30 m)

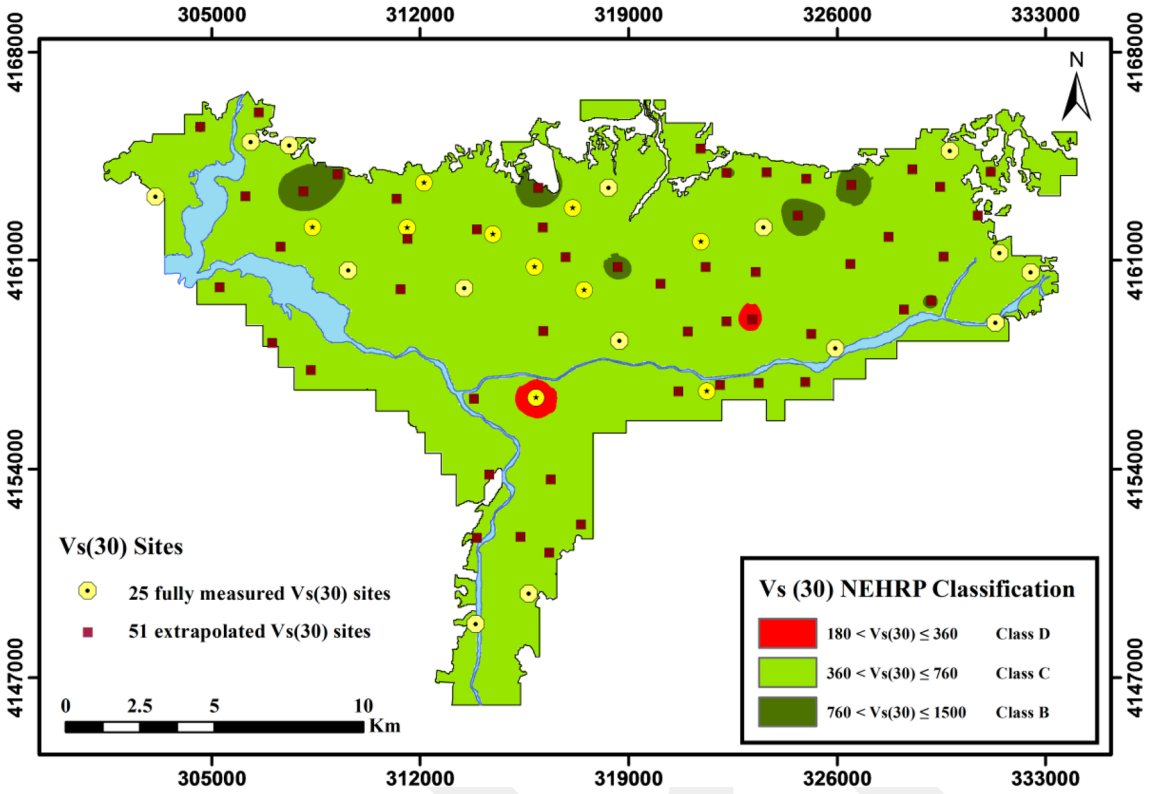

Fig. 9 Mean V_{S30} map for Kahramanmaras city

Comparing the V_{S30} values obtained by means of the MASW and MAM tests and those estimated using empirical relationships already available in the literature provides testing the use of V_S values as input data in the ground response analyses. For this purpose, various SPT-based empirical correlations proposed by Iyisan (1996), Hasancebi and Ulusay (2007), Dikmen (2009), Akin et al. (2011), and Kirar et al. (2016) have been investigated to compile the V_S based SSC maps in the study area. The previous SPT-N versus V_S relations were used to substitute SPT-N values of the study area in the formulas to propose V_S values as a function of SPT-N values, and then to produce V_{S30} maps. The inserted values of SPT-N in these relationships were the data extracted from the fieldwork carried out in the study area at 287 boreholes. Table 2 gives a summary of the proposed approaches by these researchers. Recently developed SPT-N-based *Vs* values were utilized to generate V_{S30} maps and classifications based on NEHRP system over the study area, although the regressions previously developed were made to correlate the SPT-N values into V_S. According to Dikmen (2009) and Akin et al. (2011), the study area has been entirely classified as class D, whilst Hasancebi and Ulusay (2007) classified the same area as dominantly D with small zones of class C. However, the area has been dominantly classified as C with small zones of class D by Iyisan (1996) and Kirar et al. (2016). As can be seen from Fig. 11, there are discrepancies among the V_{S30} maps produced using Kriging technique by different researchers. In the light of the studies by Iyisan (1996) conducted by means of cross-hole and down-hole seismic techniques, Hasancebi and Ulusay (2007) carried out by seismic refraction test, Kirar et al. (2016) by the MASW and SPT tests, Dikmen (2009) CPT, SCPT and ReMi methods, and Akin et al. (2011) by SPT-based uphole tests at different locations and various soil types, the authors' interpretation is that such differences could be attributed to some parameters employed in the regression analyses including depth, geological structure, stratigraphy, age of geological units, density, grain size distribution, fines content, effective stress, bedrock level, the accuracy of the SPT values, and number of data employed in those researches.

An interpolated map has also been generated to verify the works undertaken for average V_S at shallow 5 m as illustrated in Fig. 12. As can be seen from the figure, the central part of the study area belongs to class D to indicate the presence of stiff soils (180 m/s $< V_S \leq$ 360 m/s). Accordingly, one can recognize the similarity of having the highest risky zones in the middle part of the city which is the alluvial sediments. The dark green zones in Fig. 12 indicate the presence of very strong soil in the northern

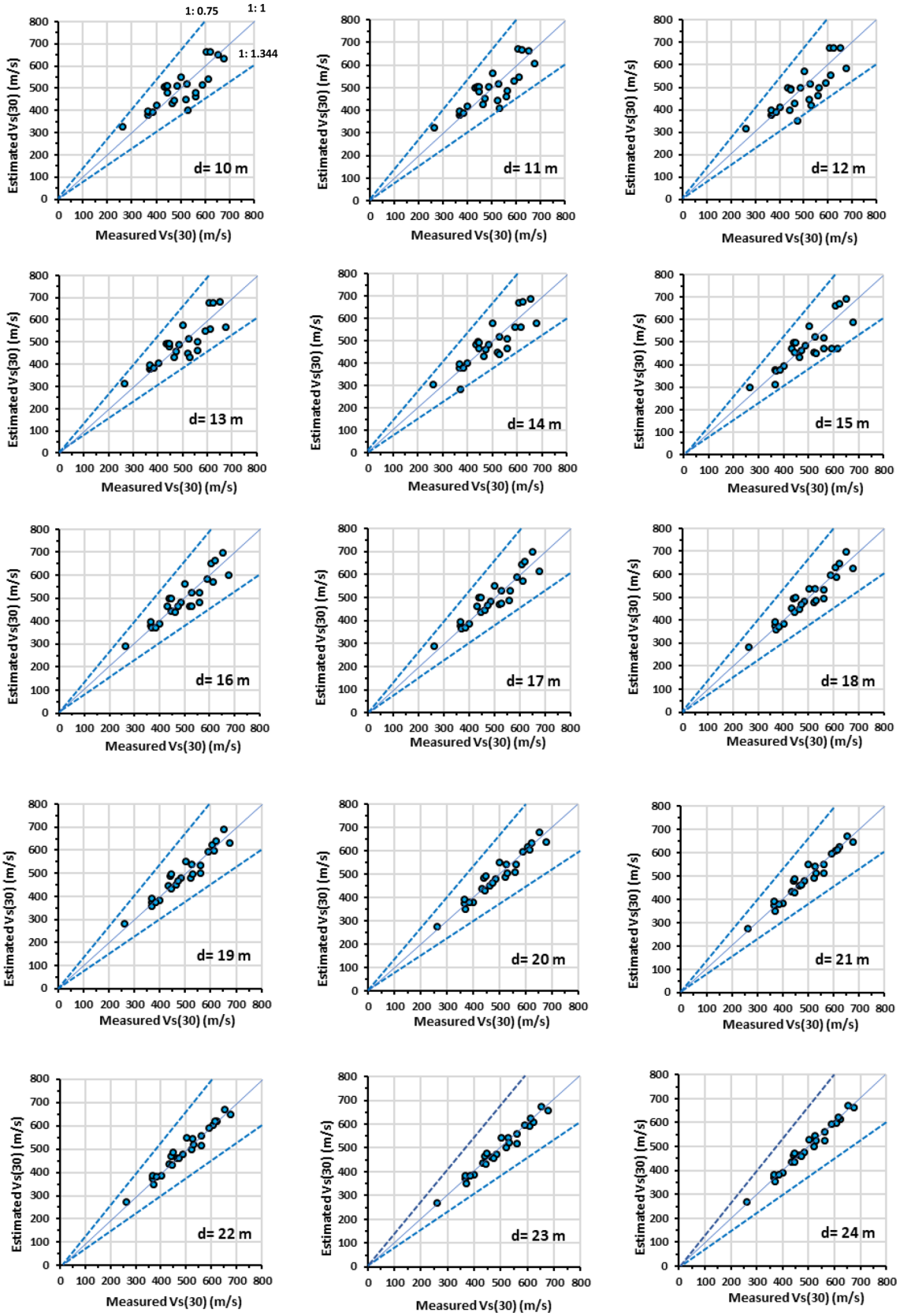

Fig. 10 Comparison of estimated V_{S30} versus measured V_{S30} of the 25 sites for the mentioned depths bounded by the lines of 1:0.75, 1:1 and 1:1.344

Table 2 Summary of the proposed relationships

Researcher	V_S (m/s), All Soils	R^2 or R
Iyisan (1996)	$V_S = 51.5 \times N^{0.516}$	$R = 0.81$
Hasancebi and Ulusay (2007)	$V_S = 90 \times N^{0.308}$	$R = 0.73$
Dikmen (2009)	$V_S = 58 \times N^{0.39}$	$R = 0.75$
Akin et al. (2011)	$V_S = 59.44 \times N^{0.109} \times z^{0.426}$	$R = 0.89$
Kirar et al. (2016)	$V_S = 99.5 \times N^{0.345}$	$R^2 = 0.80$

part of the study area. The difference between the V_{S30} map and the V_{S5} map may be explained due to the presence of very dense soil or soft rock below the stiff soil for the shallow 30 m depth.

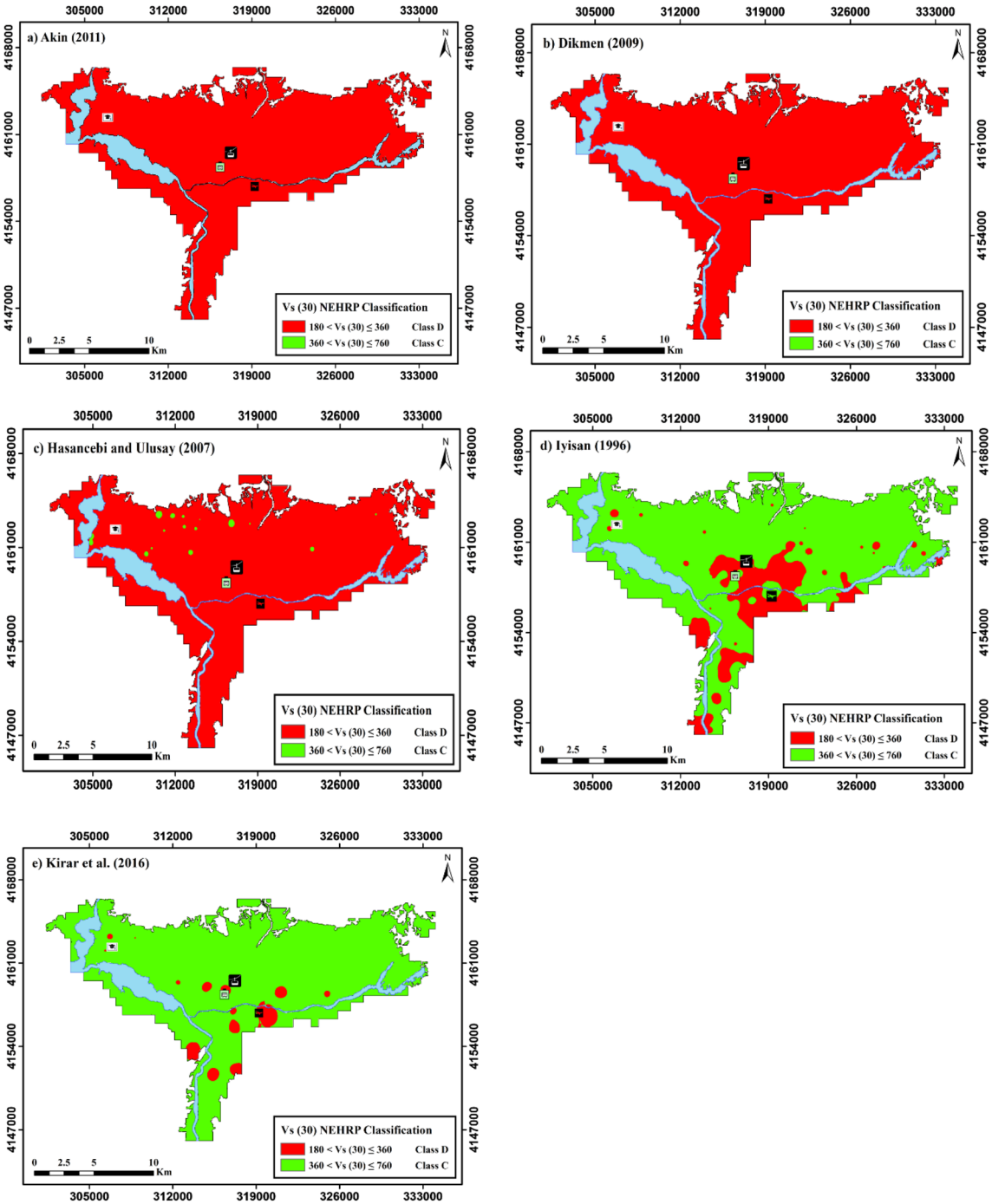

Fig. 11 SSC on the basis of V_{S30} as a function of SPT-N as estimated from the previous studies

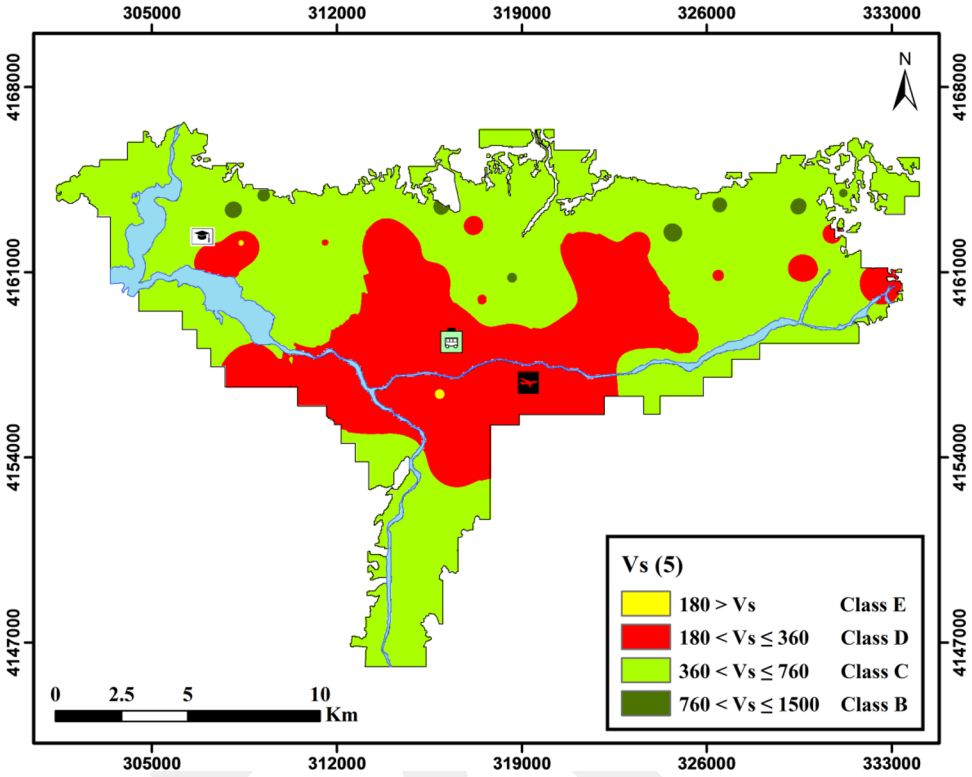

Fig. 12 Average V_S values for the shallow 5 m of Kahramanmaras city

Validation of the equations

To set the predictive ability of the derived equations for V_{S30} values, a comparison between V_{S30} measured (V_{SM}) and V_{S30} estimated (V_{SE}) is required as a validation procedure, which would be carried out by means of the Root Mean Square (RMS) value. Diagrammatic validations have been applied to analyse the relations for the depths ranging from 10 to 24 m. Demonstrative procedures for residual analysis have been performed to compare the V_{SM} and V_{SE} values. Here in the present study, two graphical techniques have been employed to set the accuracy of the generated

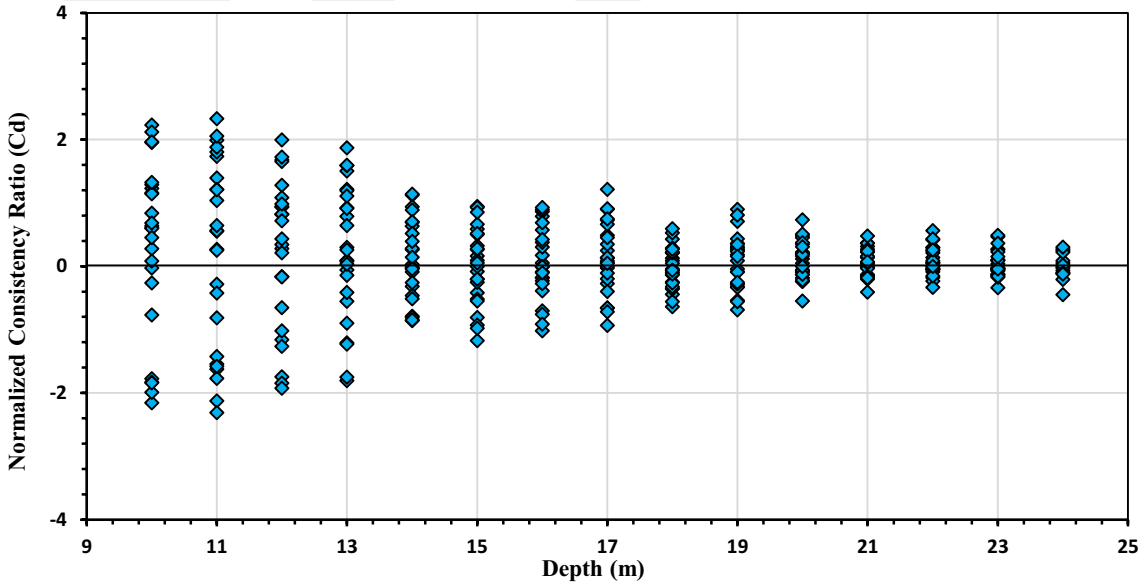

Fig. 13 Variance of C_d for the proposed 15 formulas with depth

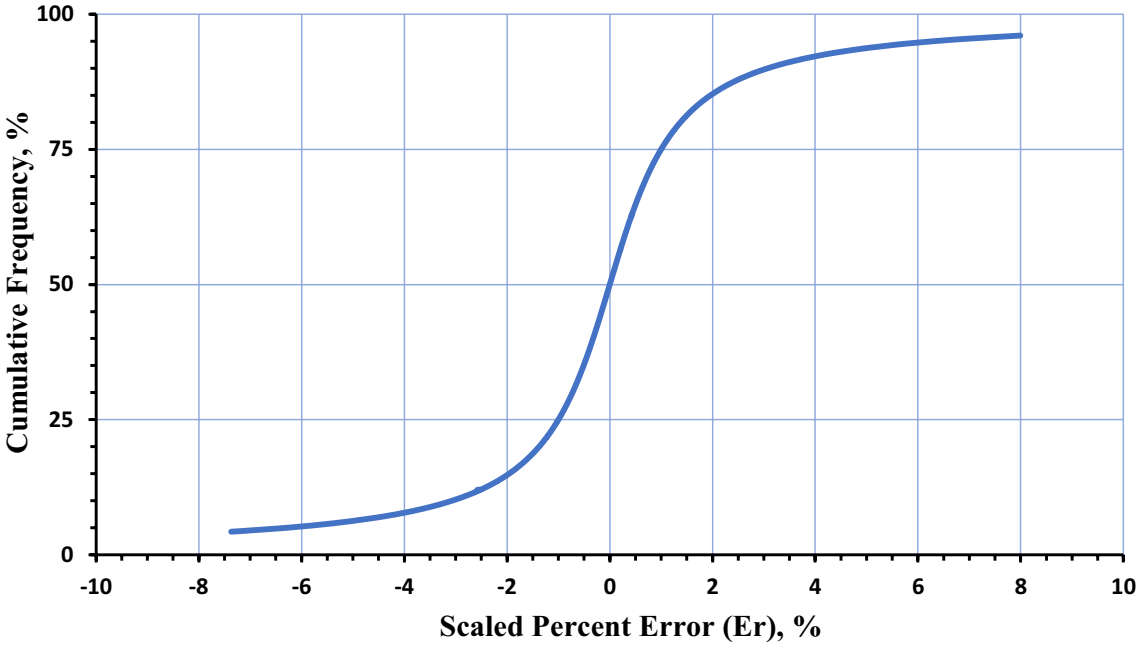

Fig. 14 Scaled proportional inaccuracy of V_S predicted with the measured velocity

correlations. The first approach studied was the ratio of normal consistency (C_d) (Dikmen 2009).

$$C_d = \frac{V_{SM} - V_{SE}}{d} \tag{5}$$

where C_d is the normal consistency ratio, V_{SM} is the measured V_{S30} in 25 sites on the study area, V_{SE} is the estimated V_{S30} by means of Eq. 4, and d is depth. Figure 13 presents the dispersion in the normalized consistency ratio (C_d) with depth. The mean value of C_d converges to zero with an increment in depth. This proves a good agreement between the estimated and measured (actual) data in the prediction of V_{S30}. More than 50% of the sites in the study area have positive values of C_d, which indicates an underestimation for the estimated V_{S30} values. According to the method employed in this study, the error range was found to be around 2.4%, an insignificant value for velocity estimates extending up to 24 m.

Another technique to examine the accuracy of the derived equations was the scaled percent error E_r as follows (Dikmen 2009; Anbazhagan et al. 2013).

$$E_r = 100\frac{V_{SE} - V_{SM}}{V_{SE}} \tag{6}$$

where E_r is the scaled percent error a measure of proximity between two values, V_{SM} and V_{SE} are the measured (actual) and estimated V_{S30} in values, respectively. Figure 14 shows the scaled proportional inaccuracy variation for the new relations and clarified that 96% of the data was found to be within an 8% error of margin denoting a better calculation of shear wave velocity by theoretically proposed formulas.

Conclusion

Due to the seismic activities in Kahramanmaras in Turkey, a study had been found to be required to demonstrate the effect of site conditions on amplifying/attenuating possible seismic waves in the study area. Hence, the aim of the present study was to make an accurate seismic site classification (SSC) study in Kahramanmaras city with a population of more than a million people. Soil profile as well as the SSC in the study area was obtained using the geophysical investigations and the boreholes drilled to perform Standard Penetration Tests (SPT). Analyses of the SSC based on V_{S30} values were mapped by means of a Geographical Information System (GIS) based computer software. A 15 empirical correlations based on the study by Boore (2004) have been proposed for the sites without V_S at upper 30 m depth to generate a series of SSC maps based on the NEHRP. Validation of each proposed correlation made using both the RMS and E_r approaches revealed that the estimated V_{S30} values and the measured (actual) V_{S30} values were found to be in a good agreement varying from $R^2 = 0.67$ to $R^2 = 0.95$, particularly in larger depths. Accordingly, the study area was predominantly classified as soil class C with about 78% of the area, while the small areas were rarely classified as soil class B with about 14% of the area, and D with about 8% of the whole area. Evidently, the approach on extending V_S

values up to 30 m depth, and the complied GIS maps could be effectively used by researchers and engineers for further studies on the purpose of land-use planning and urban development, as well as earthquake hazard estimates.

Data and resources The Global Centroid Moment Tensor Project database was searched using www.globalcmt.org/CMTsearch.html (last accessed May 2019).

References

Akil B, Ecemis BY (2011) Geological-Geotechnical study report for the municipality of Kahramanmaras, Directorate of Underground Studies Department

Akin MK, Kramer S, Topal T (2011) Empirical correlations of shear wave velocity (Vs) and penetration resistance (SPT-N) for different soils in an earthquake-prone area (Erbba-Turkey). Eng Geol 119:1–17

Akin MK, Kramer S, Topal T (2013) A newly developed seismic microzonation model of Erbaa (Tokat, Turkey) located on seismically active easternsegment of the North Anatolian Fault Zone (NAFZ). Nat Hazards 65:1411–1442

Ambraseys NN, Jackson JA (1998) Faulting associated with historicaland recent earthquakes in the eastern Mediterranean region. Geophys J Int 133:390–406

Anbazhagan P, Kumar A, Sitharam TG (2013) Seismic site classification and correlation between standard penetration test N value and shear wave velocity for Lucknow City in Indo-Gangetic Basin. Pure Appl Geophys 170:299–318

Biricik AS, Korkmaz H (2001) The Seismicity of Kahramanmaras Eastern Mediterranean-TURKEY. Marmara Coğrafya Dergisi 1:53–82

Boore DM (2004) Estimating Vs (30) (or NEHRP Site Classes) from shallow velocity models (Depths 30 m). Bull Seismol Soc Am 94:591–597

Boore DM, Joyner WB, Fumal TE (1997) Equations for estimating-horizontal response spectra and peak acceleration from western North American earthquakes: a summary of recent work. Seism Res Lett 68:128–153

Boore DM, Thompson EM, Cadet H (2011) Regional correlations of V_{S30} and velocities averaged over depths less than and greater than 30 meters. Bull Seismol Soc Am 101:3046–3059

Borcherdt RD (1994) Estimates of site dependent response spectra for design (methodology and justification). Earthquake Spectra 10:617–653

Building Seismic Safety Council, BSSC (2001) NEHRP recommended provisions for seismic regulations for new buildings and other structures, 2000 Edition, Part 1: Provisions, prepared by the Building Seismic Safety Council for the Federal Emergency Management Agency(Report FEMA 368), Washington, DC

Building Seismic Safety Council, BSSC (2003) NEHRP recommended provisions for seismic regulations for new buildings and other structures (FEMA 450), Part1: Provisions, prepared by the Building Seismic Safety Council for the Federal Emergency Management Agency(Report FEMA 368), Washington, DC

Choon B (2000) User's Manual for Multichannel analysis of Surface Waves, Kansas Geological Survey

Dikmen U (2009) Statistical Correlations of shear wave velocity and penetration resistance for soils. J Geophys Eng 6:61–72

Dobry R, Borcherdt RD, Crouse CB, Idriss IM, Joyner WB, Martin GR, Power MS, Rinne EE, Seed RB (2000) New site coefficient and site classification system used inrecent buildingcode provisions. Earthquake Spectra 16:41–67

Federal Emergency Management Agency of the US Department of Homeland Security, FEMA (2010) Earthquake-Resistant Design Concepts, FEMA P-749, Washington, DC

General Directorate of Disaster Affairs, Ministry of Public Works and Settlement of Turkey, GDDA (2019) Seismic Hazard Map of Turkey, Ankara

Goh ATC, Zhang WG (2014) An improvement to MLR model for predicting liquefaction-induced lateral spread using multivariate adaptive regression splines. Eng Geol 170:1–10

Gul M, Darbas G, Gurbus K (2005) Tectono-Stratigraphic position of Alacik Formation (Latest Middle Eocene–Early Miocene) in the Kahramanmaras Basin. In: Turkish with English abstract and summary, Istanbul University Mühendislik Fakültesi Yerbilimleri Dergisi 18:183–197

Hasancebi N, Ulusay R (2007) Empirical correlations between shear wave velocity andpenetration resistance for ground shaking assessments. Bull Eng Geol Env 66:203–213

Husing SK, Zachariasse WJ, Hinsbergen DJJ, Krijgsman W, Inceoz M, Harzhauser M, Mandic O, Kroh A (2009) Oligocene-Miocene basin evolution in SE Anatolia, Turkey: constraints on the closure of the eastern Tethys gateway. Geol Soc London 311:107–132

Iyisan R (1996) Correlations between shear wave velocity and in-situ penetration test results, Chamber of Civil Engineers of Turkey. Teknik Dergi 7:1187–1199 (**in Turkish**)

Kanli AI, Tildy P, Pronay Z, Pinar A, Hemann L (2006) Vs30 mapping and soil classification for seismic site effect evaluation in dinar region, SW Turkey. Geophys J Int 165:223–235

Karig DE, Kozlu H (1990) Late Palaeogene-Neogene evolution of the triple junction regionnear Maras, south-central Turkey. J Geol Soc 147:1023–1034

Kirar B, Maheshwari BK, Muley P (2016) Correlation between shear wave velocity (V_S) and SPT resistance (N) for Roorkee region. Int J Geosynth Ground Eng 2:9

Korkmaz H (2000) Geomorphology of Kahramanmaras Basin. PhD Thesis, Marmara University, Istanbul, Turkey

Leparoux D, Bitri A, Grandjean G (2000) Underground cavities detection: a new method based on seismic Rayleigh waves. Euro J Environ Eng Geophys 5:33–53

Nalbant SS, McCloskey J, Steacy S, Barka AA (2002) Stress accumulation and increasedseismic risk in eastern Turkey. Earth Planet Sci Lett 195:291–298

Ozmen TO, Yamanaka H, Alkan MA, Ceken U, Ozturk T, Sezen H (2017) Microtremor array measurements for shallow S-wave profiles at strong-motion stations in Hatay and Kahramanmaras Provinces, Southern Turkey. Bull Seismol Soc Am 107:445–455

Palutoglu M, Sasmaz A (2017) 29 November 1795 Kahramanmaras Earthquake, Southern Turkey. Bull Miner Res Explor 155:191–206

Park CB, Miller RD, Xia J (1999) Multichannel analysis of surface waves. Geophysics 64:800–808

Perincek D, Kozlu H (1984) Stratigraphy and Structural Relations of the Units in the Afşin-Elbistan-Doğanşehir Region (Eastern Tauros), Geology of Tauros Belt, MTA. pp 181-198

Pitilakis K (2004) Site effects. In: Ansal A (ed) recent advances in earthquake geotechnical engineering and microzonation, vol 368. Kluwer Academic Publications, Netherlands, pp 139–197

Rodriguez-Marek A, Bray JD, Abrahamson NA (2001) An empirical geotechnical seismic site response procedure. Earthq Spectra 17:65–87

Seed HB, Idriss IM, Arango I (1981) Evaluation of liquefaction potential using field performance data. J Geo Eng 109:458–482

Sengor AMC, Yilmaz Y (1981) Tethyan evolution of Turkey; a plate tectonic approach. Tectonophysics 75:181–241

Sengor AMC, Gorur N, Saroglu F (1985) Strike-slip faulting and related basin formation in zones of tectonic escape: Turkey as a case study. Soc Econ Paleontol Mineral 37:227–264

Thitimakorn T, Channoo S (2012) Shear wave velocity of soils and NEHRP site classification map of Chiang Rai City, Northern Thailand. Electron J Geotech Eng 17:2891–2904

Thompson EM, Wald DJ (2016) Uncertainty in V_{s30}-based site response. Bull Seismol Soc Am 106(2):453–463

Wengang Z, Liang H, Zixu Z, Yanmei Z (2020) Digitalization of mechanical and physical properties of Singapore Bukit Timah Granite Rocks based on borehole data from four sites. Undergr Space. https://doi.org/10.1016/j.undsp.2020.02.003

Wills CJ, Petersen M, Bryant W, Reichle M, Saucedo G, Tan S, Taylor G, Treiman J (2000) A site-condition map for California based on geology and shear-wave velocity. Bull Seismol Soc Am 90:S187–S208

Yilmaz Y (1993) New evidence and model on the evolution of the southeast Anatolian Orogeny. Geol Soc Am Bull 105:251–271

Yilmaz H, Over S, Ozden S (2006) Kinematics of the East Anatolian Fault Zone between Türkoglu (Kahramanmaras) and Celikhan (Adiyaman), eastern Turkey. Earth Planets Space 58:1463–1473

Zhang W, Goh ATC (2015) Evaluating seismic liquefaction potential using multivariate adaptive regression splines and logistic regression. Geomech Eng 10(3):269–284

Zhang W, Goh ATC, Zhang Y, Chen Y, Xiao Y (2015) Assessment of soil liquefaction based on capacity energy concept and multivariate adaptive regression splines. Eng Geol 188:29–37

Zhang J, Xiao S, Huang HW, Zhou J (2020) Calibrating a standard penetration test based method for region-specific liquefaction potential assessment. Bull Eng Geol Env. https://doi.org/10.1007/s10064-020-01815-w

Zhu J, Wang X, Wang P, Wu Z, Kim MJ (2019) Integration of BIM and GIS: Geometry from IFC to shape file using open-source technology. Autom Constr 102:105–119